

Supplementary Information

In situ observations of structural dynamics of platinum-cobalt-hydroxide nanocatalyst under CO oxidation

Li Huang¹, Xueyang Song¹, Yue Lin², Chengyong Liu¹, Wenxue He¹, Siyu Wang¹, Zhixin Long¹, Zhihu Sun^{1,*}

¹National Synchrotron Radiation Laboratory, University of Science and Technology of China, Hefei, Anhui 230029, P. R. China

²Hefei National Laboratory for Physical Sciences at the Microscale, University of Science and Technology of China, Hefei, Anhui 230026, P. R. China

*Corresponding author. E-mail: zhsun@ustc.edu.cn.

Estimation of the Weisz–Prater criterion

From the Arrhenius-type plot of the kinetics measurement, the apparent activation energy (E_a) of the Pt2-Co/SiO₂ catalyst is 14 kJ·mol⁻¹ in the low temperature region (<343 K). This is lower than the commonly accepted value (20 kJ·mol⁻¹) where the reaction might be limited by the intraparticle diffusion, rather than by kinetic control. In order to check whether the catalytic results were influenced by intraparticle mass transfer, we estimated the Weisz-Prater criterion.¹ The Weisz-Prater criterion C_{W-P} could be calculated by:

$$C_{W-P} = \frac{r_{obs} \rho_C R_p^2}{D_{eff} C_S}, \quad (1)$$

where r_{obs} is the initial global reaction rate, ρ_C is the catalyst density, R_p is the catalyst particle radius, D_{eff} is the effective diffusivity of the reactants in the pores, and C_S is the substrate concentration on the catalyst surface. From the catalyst particle size of 100-120 mesh (1.5×10^{-4} m), the CO concentration of 1%, and the reaction rate of 3.8×10^{-3} mol·kg_{cat}⁻¹·s⁻¹, from Eq. (1) we have

$$\begin{aligned} C_{W-P} &= \frac{(3.8 \times 10^{-3} \text{ mol} \cdot \text{kgcat}^{-1} \cdot \text{s}^{-1}) \times (1.3 \times 10^3 \text{ kg} \cdot \text{m}^3) \times (1.5 \times 10^{-4} \text{ m})^2}{8.9 \times 10^{-6} \text{ m}^2 \cdot \text{s}^{-1} \times 0.45 \text{ mol} \cdot \text{m}^3} \\ &= 2.8 \times 10^{-2} \ll 1. \end{aligned}$$

The obtained $C_{W-P} = 2.8 \times 10^{-2} \ll 1$ ensures that the internal diffusion effects could be neglected during the kinetic experiments.

Details of EXAFS curve-fittings

The least-squares curve-fittings of the EXAFS data of Pt2-Co/SiO₂ were performed using the ARTEMIS module implanted in IFEFFIT.² Fittings were done in the R -space within the R -range of 1.2–3.3 Å for the $k^2\chi(k)$ functions in the k -range of 2.5–12.0 Å⁻¹. A Hanning window with window width of $dk = 1.0$ Å⁻¹ was used. The number of independent points are then $N_{ipt} = 2\Delta k \cdot \Delta R / \pi = 2 \times (12.0 - 2.5) \times (3.3 - 1.2) / \pi = 12$.

Before fitting the data of Pt2-Co/SiO₂, we fit the data of Pt foil by fixing the coordination number of nearest Pt–Pt bond and the amplitude reduction factor S_0^2 was allowed to vary. This yielded the best-fit value of $S_0^2 = 0.84$. Then the S_0^2 was fixed at this value when fitting the EXAFS data of catalyst samples. For fitting the EXAFS data of Pt2-Co/SiO₂ collected at 300 K in the He and CO + O₂ atmosphere, two coordination

pairs of Pt–Pt and Pt–Co were included, because no sign of surface oxidization could be observed from both XANES and EXAFS spectra. For each pair, the coordination number N , interatomic distance R , Debye-Waller factor σ^2 , and edge-energy shift ΔE_0 were treated as adjustable parameters. The number of adjustable parameters is $N_{\text{para}} = 4 + 4 = 8$, less than $N_{\text{ipt}} = 12$. Inspection of the obtained parameters in Table 1 shows that the ΔE_0 's for the Pt–Pt ($\Delta E_0 = 5.7$ eV) and Pt–Co ($\Delta E_0 = 6.0$ eV) bonds are nearly unchanged in the He and CO + O₂ atmosphere. Therefore, for fitting the EXAFS data of Pt₂-Co/SiO₂ at higher temperatures, the ΔE_0 's for the same bonds were fixed in order to reduce the number of adjustable parameters and to break the strong correlation between ΔE_0 and R .

For the data collected within temperature ranges of 343–423 K, an additional Pt–O pair was considered to account for the FT peak at 1.7 Å (Fig. 3c) and three coordination pairs of Pt–O, Pt–Pt and Pt–Co were included. For each pair, the coordination number N , interatomic distance R , and Debye-Waller factor σ^2 were treated as adjustable parameters. ΔE_0 was also an adjustable parameter. Besides, for the data collected at 423 K, a common third cumulant C_3 for the Pt–Pt and Pt–Co bonds were included to account for the anharmonicity of the interatomic potential. The total number of adjustable parameters is $N_{\text{para}} = 4 + 3 + 3 + 1 = 11$, or $N_{\text{para}} = 4 + 3 + 3 = 10$, less than $N_{\text{ipt}} = 12$.

For the data collected at 473 K, the two-shell model including a Pt–O and a Pt–Pt pair is sufficient to give a satisfactory match. Therefore, the number of adjustable parameters is $N_{\text{para}} = 4 + 3 + 1 = 8 < N_{\text{ipt}}$.

With the strategies, the curve-fitting results for Pt₂-Co/SiO₂ under various conditions are shown in Figure S5 and the parameters are listed in Table 1. All the yielded R -factors are not larger than 0.01, indicating the good fitting qualities.

Supplementary Figures

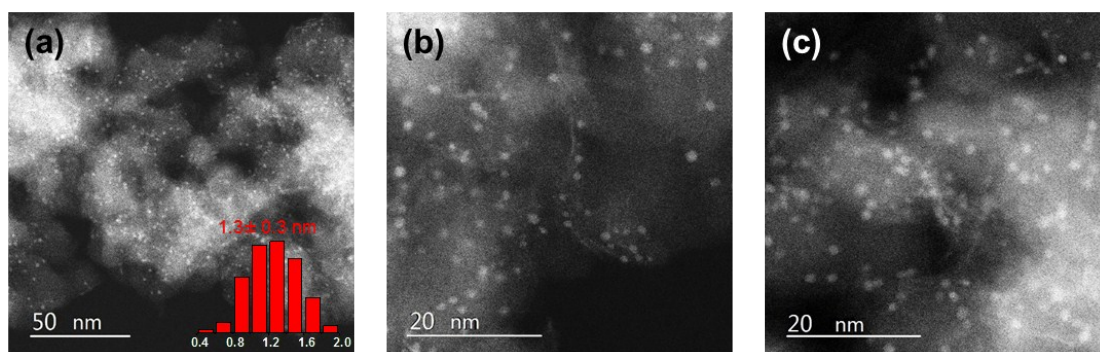


Figure S1. Aberration-corrected HAADF-STEM images of Pt₂-Co/SiO₂ sample.

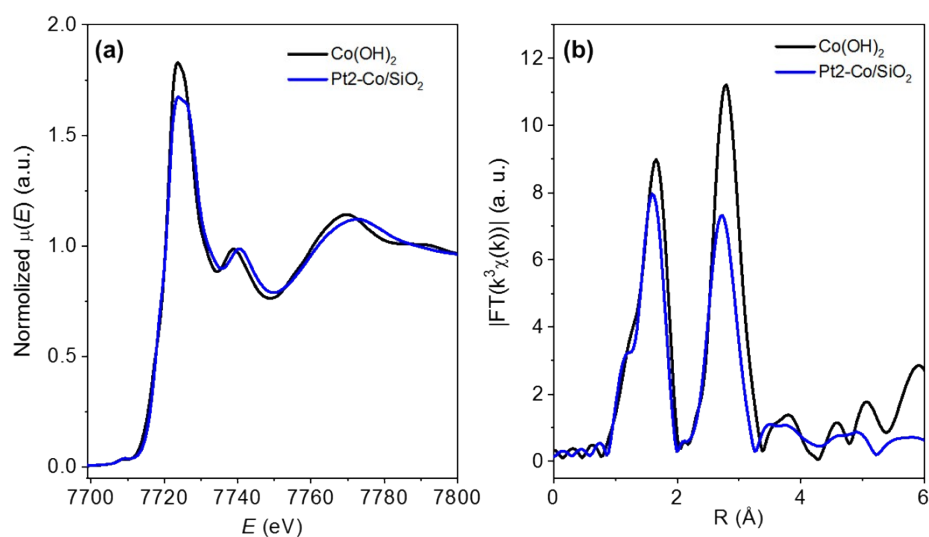


Figure S2. (a) Co K-edge XANES spectra of Pt₂-Co/SiO₂ catalysts and Co(OH)₂ bulk. (b) Their corresponding FT spectra of the $k^3\chi(k)$ functions within the k -range of 2.4-12.5 Å⁻¹.

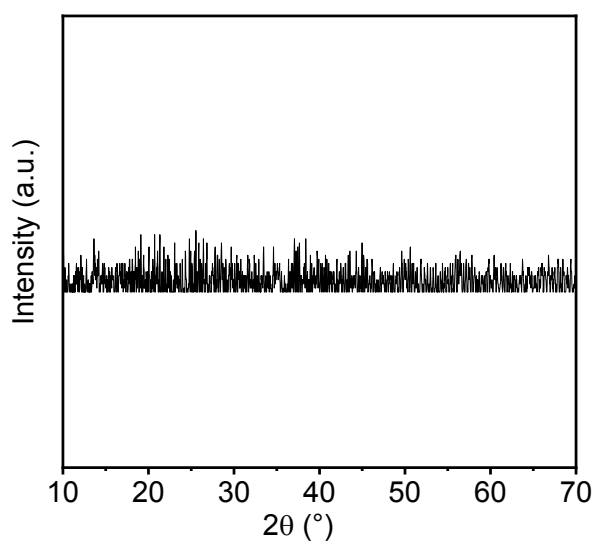


Figure S3. XRD pattern of the as-synthesized Pt₂-Co/SiO₂ catalyst.

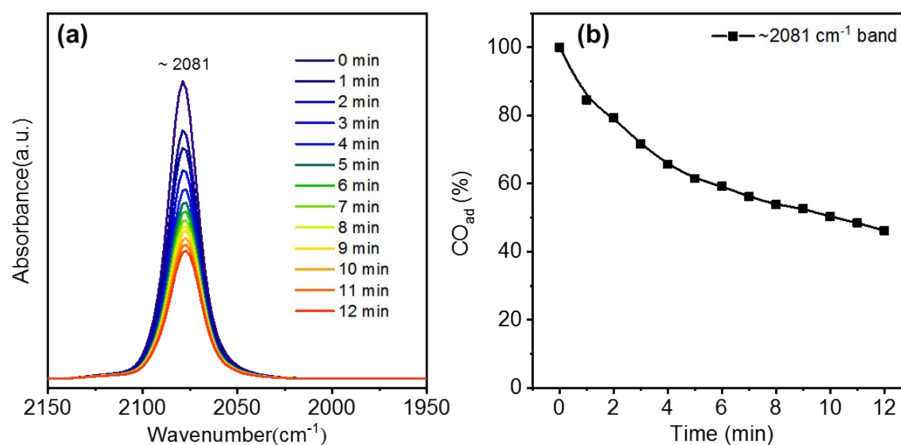


Figure S4. (a) Temporal evolutions of DRIFTS spectra for CO adsorbed on Pt/SiO₂ after O₂ injection at 300 K. (b) Percentages of integrated area of CO adsorbed on different surface sites against the oxidation time of O₂.

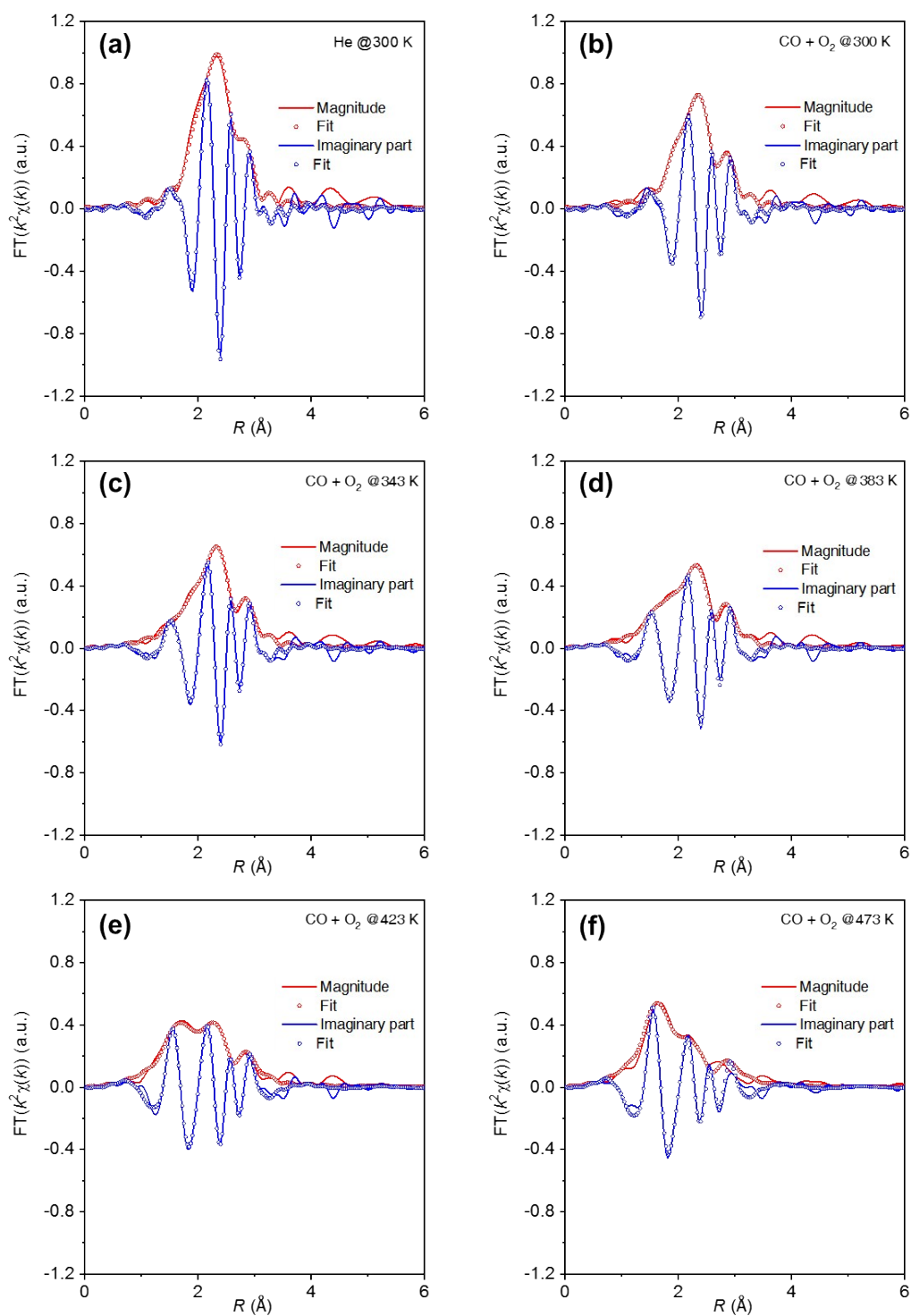


Figure S5. The curve-fitting results of the Pt₂-Co/SiO₂ sample showing the magnitude (red) and the imaginary part (blue) of the FT curves under various conditions: (a) He@ 300 K; (b) CO + O₂ @300 K; (c) CO + O₂ @343 K; (d) CO + O₂ @383 K; (e) CO + O₂ @423 K; (f) CO + O₂ @473 K.

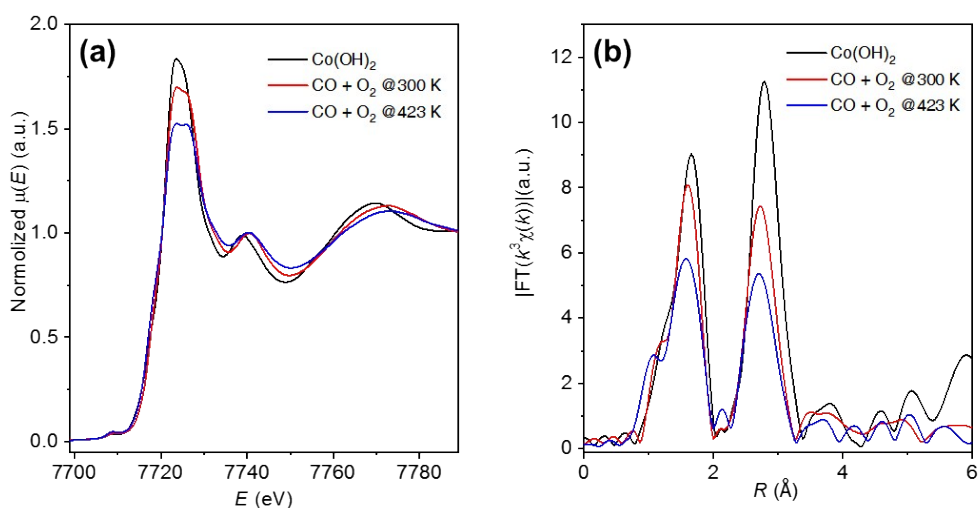


Figure S6. Comparison of the Co K -edge *in-situ* data of Pt2-Co/SiO₂ collected at 300 and 423 K under the reaction atmosphere: (a) XANES, (b) the FT curves of EXAFS.

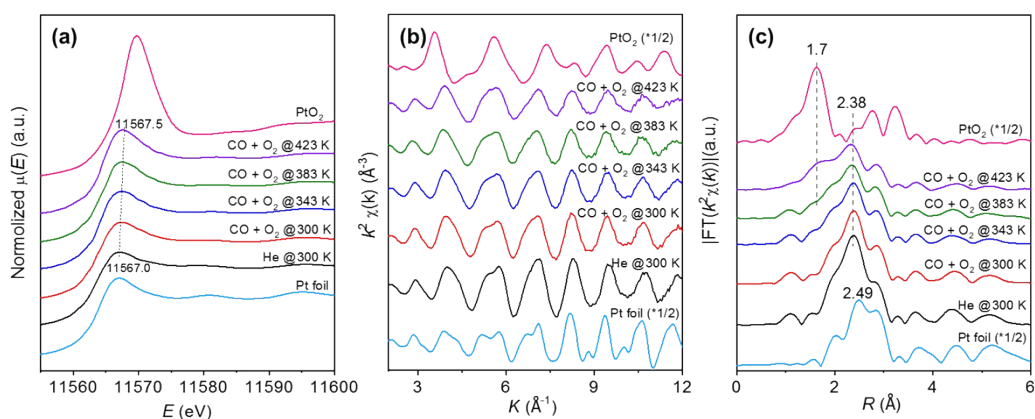


Figure S7. *In-situ* Pt L_3 -edge XAFS spectra of pre-reduced Pt1-Co/SiO₂ in the first cycle of changing conditions: in He at 300 K, and in the CO + O₂ reaction atmosphere at various temperatures. (a) XANES spectra; (b) the k^2 -weighted EXAFS oscillatory $\chi(k)$ functions, and (c) non-phase-shift-corrected R -space FT curves of the $k^2\chi(k)$ functions. For comparison, the data of Pt foil and PtO₂ bulk are also displayed.

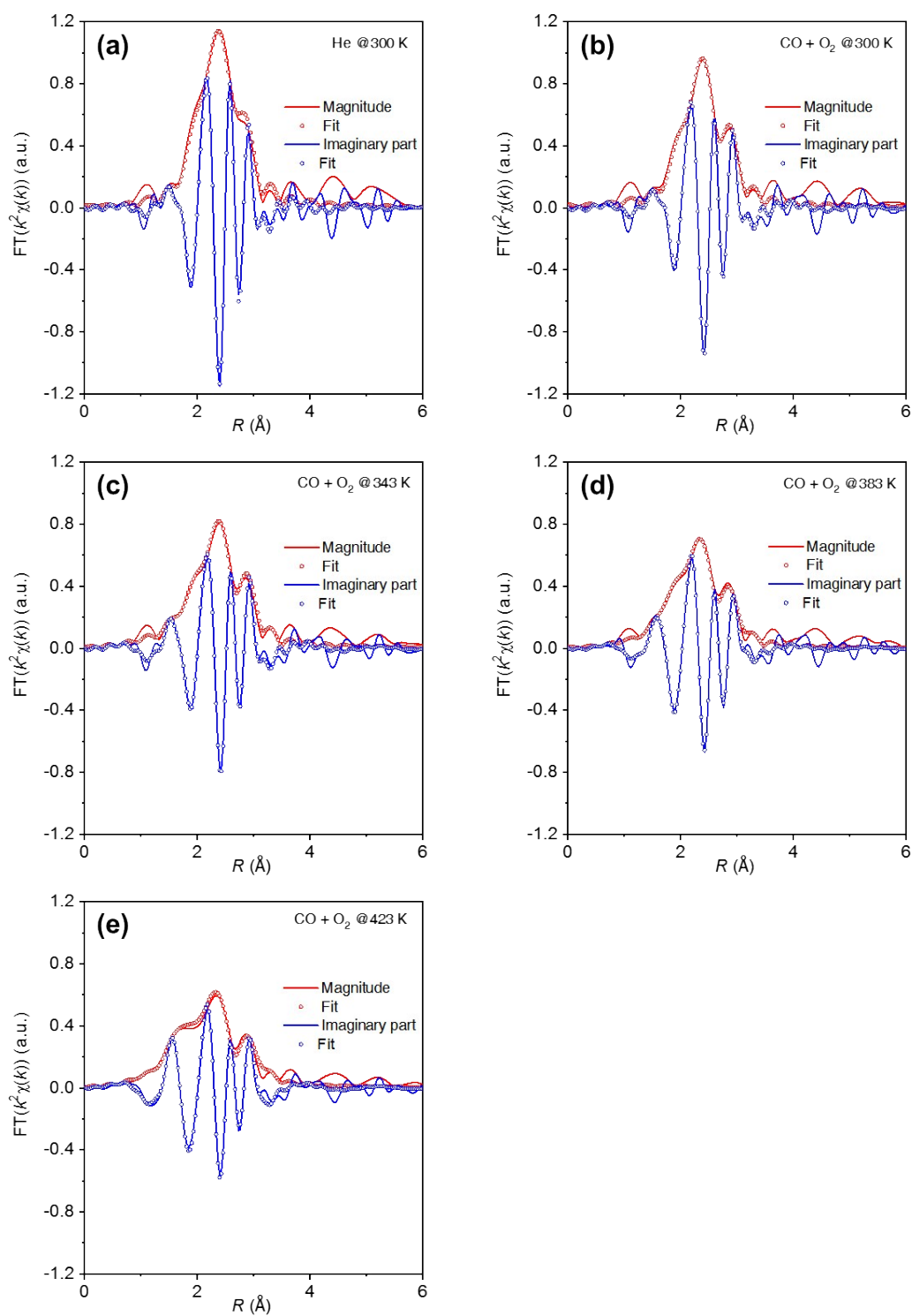


Figure S8. The curve-fitting results of the Pt1-Co/SiO₂ sample showing the magnitude (red) and the imaginary part (blue) of the FT curves under various conditions: (a) He@ 300 K; (b) CO + O₂ @300 K; (c) CO + O₂ @343 K; (d) CO + O₂ @383 K; (e) CO + O₂ @423 K.

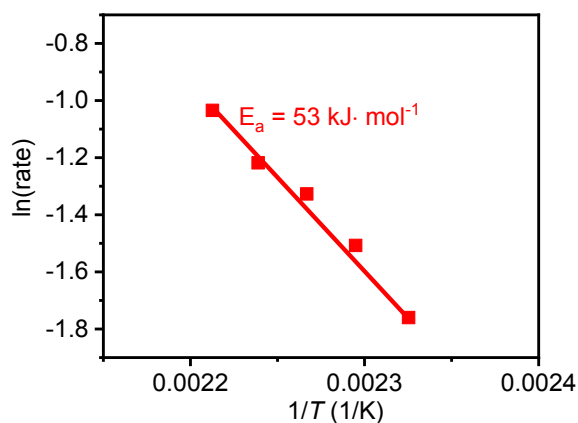


Figure S9. Arrhenius plot of the kinetics measurement at temperatures above 343 K for Pt₂-Co/SiO₂, yielding the apparent activation energy $E_a = 53 \text{ kJ} \cdot \text{mol}^{-1}$.

Table S1. Structure parameters of Pt₁-Co/SiO₂ under various conditions extracted from quantitative curve-fittings of the Pt L_3 -edge EXAFS data.

Condition	Pair	N	R (Å)	σ^2 (Å ²)	ΔE_0 (eV)	C_3 (10 ⁻⁴ Å ³)	η^*
Pt foil	Pt-Pt	12	2.77	-	-	-	-
He @300 K	Pt-Co	1.5±0.5	2.65±0.02	0.008±0.001	10.0±1.7	-	14%
	Pt-Pt	9.0±0.4	2.72±0.02	0.008±0.001	7.2±0.5	-	
CO+O ₂ @300 K	Pt-Co	1.3±0.3	2.70±0.02	0.011±0.002	10	-	13%
	Pt-Pt	9.0±0.4	2.73±0.02	0.009±0.001	7.2	-	
CO+O ₂ @343 K	Pt-O	0.3±0.2	2.02±0.03	0.005±0.004	8.3±2.0	-	11%
	Pt-Co	1.1±0.3	2.71±0.03	0.015±0.004	10	-	
	Pt-Pt	8.8±0.3	2.73±0.02	0.009±0.001	7.2	-	
CO+O ₂ @383 K	Pt-O	0.4±0.1	2.05±0.02	0.005±0.003	6.6±1.5	-	7%
	Pt-Co	0.7±0.1	2.69±0.03	0.009±0.004	10	-	
	Pt-Pt	8.8±0.3	2.74±0.02	0.011±0.001	7.2	-	
CO+O ₂ @423 K	Pt-O	0.7±0.2	2.03±0.02	0.004±0.002	6.6±1.2	-	4%
	Pt-Co	0.4±0.2	2.69±0.03	0.008±0.003	10	-	
	Pt-Pt	8.8±0.5	2.74±0.02	0.012±0.001	7.2	1.4	

* η is the extent of Pt-Co alloying, calculated by $\eta = N_{\text{Pt-Co}} / (N_{\text{Pt-Co}} + N_{\text{Pt-Pt}})$.

References

1. P. B. Weisz and C. D. Prater, in *Advances in Catalysis*, eds. W. G. Frankenburg, V. I. Komarewsky and E. K. Rideal, Academic Press, 1954, vol. 6, pp. 143-196.
2. B. Ravel and M. Newville, *J. Synchrotron Rad.*, 2005, **12**, 537-541.